

Chapter 34

Penetration of Magnetospheric Electric Fields to the Low Latitude Ionosphere During Storm/Substorms

Takashi Kikuchi, Kumiko K. Hashimoto, Atsuki Shinbori, Yuji Tsuji, and Shin-Ichi Watari

Abstract Penetration of the magnetospheric electric fields to low latitude ionosphere is examined using magnetometer data from high latitude to the dip equator during substorms and geomagnetic storms. To detect the penetration electric fields, we analyzed magnetic disturbances at the dip equator, subtracted by those at low latitude (DP2). During substorm growth phase, the DP2 currents are enhanced by the dawn-to-dusk convection electric field, which are supplied by the Region-1 field-aligned currents (R1 FACs) via the mid and low latitude ionosphere. On the other hand, the DP2 currents decrease significantly during the substorm expansion, superposed by reversed currents flowing from the R2 FACs. In particular, when the IMF turns northward during the substorm, the DP2 currents change to the counter-electrojet (CEJ), i.e., overshielding currents at the dip equator. During the storm main phase, the DP2 currents are very much intensified by the enhanced convection electric field. However, the DP2 currents change to the CEJ at the beginning of the storm recovery phase. The overshielding electric field as well as the convection electric field causes dramatic changes in the low latitude ionosphere.

34.1 Convection Electric Field and Global DP2 Currents

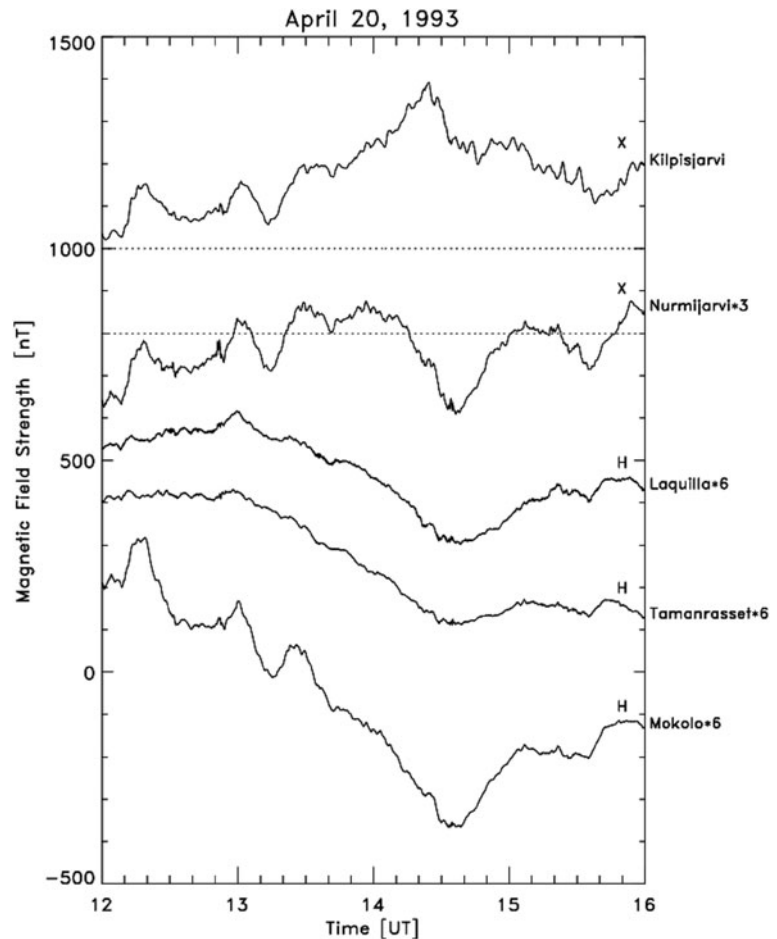
The magnetospheric convection is generated by the reconnection between the interplanetary magnetic

field (IMF) and the Earth's magnetic field at the magnetopause (Dungey, 1961). Global MHD simulations have provided detailed structures of a dynamo generating the Region 1 field-aligned currents (R1 FACs), which is located around the cusp where the solar wind energy is converted to the thermal energy of high pressure plasma and generates the convection electric field and the R1 FACs (Tanaka, 1995, 2007; Siscoe et al., 2000). The R1 FACs flow into/out from the polar ionosphere in the morning/afternoon sector (Iijima and Potemra, 1976, 1978).

The convection electric field causes DP2 magnetic fluctuations at high latitude and dip equator (Nishida et al., 1966; Nishida, 1968a, b; Kikuchi et al., 1996; Kobea et al., 1998). The DP2 fluctuations were coherent with variations in the southward IMF, suggesting direct penetration of the magnetospheric electric field to the dip equator (Nishida, 1968b). Kikuchi et al. (1996), as shown in Fig. 34.1, demonstrated that the DP2 fluctuations observed at afternoon auroral latitude (Kilpisjärvi) during the growth phase of a substorm (1200–1400 UT) are coherent with those at mid latitude (Nurmijärvi) and dip equator (Mokolo) with a correlation coefficient of 0.9 and no time shift greater than 25 s. During the DP2 fluctuation event, EISCAT measured the convection electric field and height-integrated Hall and Pedersen conductivities. The Hall current calculated from these parameters well agrees with the DP2 fluctuations at Kilpisjärvi located near EISCAT. The high coherency between high latitude and equator implies that the convection electric field was transmitted to the equator near-instantaneously, driving the Pedersen current amplified by the Cowling effect at the dayside dip equator (Hirono, 1952; Baker and Martyn, 1953). As a result, the DP2 decreases with decreasing latitude, but increases at the dip equator

T. Kikuchi (✉)
Solar-Terrestrial Environment Laboratory, Nagoya University,
464-8601 Nagoya, Aichi, Japan
e-mail: kikuchi@stelab.nagoya-u.ac.jp

Fig. 34.1 The X-component at the IMAGE stations, Kilpisjarvi (65.76° CGM Lat), Nurmijarvi (56.79° CGM Lat), and the H-component at Laquilla (36.19° CGM Lat), Tamanrasset (5.86° CGM Lat) and Mokolo (−1.5° Dip Lat) for the time interval of 12–16 UT on April 20, 1993. The dotted lines for the IMAGE stations indicate the quiet nighttime level. The data are multiplied by a factor of 3 for Nurmijarvi and 6 for the mid to equatorial latitudes for the sake of a better comparison of the wave forms (figure 2 of Kikuchi et al. (1996), reproduced by permission of American Geophysical Union)



with an equatorial to low latitude amplitude ratio of 4 (Nishida, 1968a). The DP2 is different from the DP1 associated with the auroral electrojet intensified during the substorm expansion phase (Nishida, 1968a). The equatorial enhancement of geomagnetic perturbations is an important feature of the equatorward extension of ionospheric currents driven by the potential electric field in the polar ionosphere. Thus, the equatorial DP2 is connected with the R1 FACs via the Pedersen currents at mid and low latitude (Kikuchi et al., 1996).

The diurnal magnetic variation at the geomagnetic equator is often depressed substantially during disturbed periods (Matsushita and Balsley, 1972; Onwumechilli et al., 1973; Kikuchi et al., 1996). Matsushita and Balsley (1972) critically discussed that the DP2 fluctuations should be measured negatively from the quiettime level. However, the DP2 should be measured positively from the smoothed diurnal variation, because of the high coherency between the high

latitude and equator with time shift of 2 min (Nishida, 1968b) and 25 s (Kikuchi et al., 1996). The depression of the diurnal variation may be caused by a westward electric field due to the disturbance dynamo (Blanc and Richmond, 1980).

34.2 Overshielding Electric Field and CEJ

The enhanced convection electric field drives an earthward motion of plasma in the plasmasheet, generating a partial ring current and the Region-2 field-aligned currents (R2 FACs) in the inner magnetosphere. The R2 FACs build up an electric field in the ionosphere with an opposite direction to that of the convection electric field at mid and low latitudes (Vasyliunas, 1972; Jaggi and Wolf, 1973; Southwood, 1977; Senior and Blanc, 1984). The R2 FACs provide a northward

electric field at auroral latitude and southward electric field at mid latitude in the afternoon sector. As a result, the eastward auroral electrojet intensifies, but the eastward current reduces at subauroral-mid latitudes. In other words, the electric field associated with the R2 FACs tends to cancel the convection electric field, i.e., shielding works at lower latitude. The time constant of the shielding has been estimated as 17–20 min from the magnetometer observations (Somayajulu et al., 1987; Kikuchi et al., 2000) and 20–30 min from the theoretical calculations (Senior and Blanc, 1984; Peymirat et al., 2000).

When the convection electric field reduces abruptly because of the northward turning of the IMF, the electric field reverses its direction at mid-equatorial latitudes. The reversal of the penetrated electric field was observed by the Jicamarca incoherent scatter radar at the equator, which was identified as the overshielding electric field (Kelley et al., 1979; Gonzales et al., 1979; Fejer et al., 1979). The reversed current at the equator appears as the counter-electrojet (CEJ) (Rastogi and Patel, 1975; Rastogi, 1977, 1997; Koba et al., 2000; Kikuchi et al., 2000, 2003). The equatorial CEJ is connected with the R2 FACs via the auroral ionosphere.

34.3 DP2 Currents and CEJ During Substorms

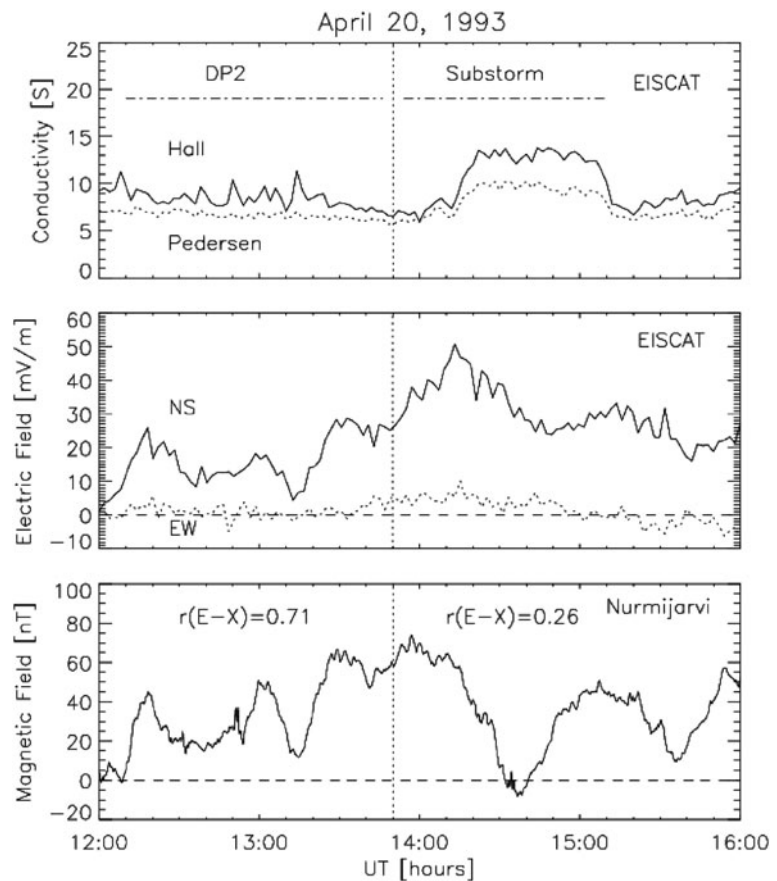
The substorm growth phase is initiated by the southward turning of the IMF, which causes DP2 currents in the ionosphere (Iijima and Nagata, 1972; Nishida and Kamide, 1983; Kamide et al., 1996). Kikuchi et al. (1996, 2000) demonstrated that the eastward ionospheric currents increased at auroral-mid latitudes in the afternoon sector, coherently with an enhancement of the EEJ during the substorm growth phase (1200–1400 UT, Fig. 34.1). However, the coherency between the auroral (Kilpisjärvi) and mid latitude (Nurmijärvi) broke down during the substorm expansion phase (1400–1510 UT, Fig. 34.1). Figure 34.2 shows the height-integrated Hall (solid curve in the upper panel) and Pedersen (dotted curve) conductivities, northward (solid curve in the middle panel) and eastward (dotted curve) electric fields measured by EISCAT, and the X-component magnetic field at Nurmijärvi measured from the quiettime diurnal variation during the

growth phase (DP2 in the upper panel) and expansion phase of the substorm (Kikuchi et al., 2000). Under an assumption that the convection electric field at EISCAT penetrated to Nurmijärvi with geometrical attenuation (factor = 0.4) and the R2 FACs developed between the two latitudes and increased/decreased the electric field at the auroral/mid latitude, the convection and shielding electric fields are derived from these parameters. Figure 34.3 (upper panel) shows the convection electric field, E_1 (solid line) and shielding electric field, E_2 (dashed line) at auroral latitude (EISCAT). The shielding electric field is in the same direction as the convection electric field, intensifying the electric field at auroral latitude. Figure 34.3 (lower panel) shows that the convection electric field decreases to be $E_1 \times 0.4$ at mid latitude (Nurmijärvi) because of the geometrical attenuation, while the shielding electric field is $-E_2$ with an opposite direction to the convection electric field. During the growth phase before 14 UT, the convection electric field is dominant, but the shielding electric field increased significantly during the expansion phase after 1400 UT. Thus, the shielding electric field reduces the electric field at mid latitude, causing the overshielding when E_2 is greater than $E_1 \times 0.4$ at around 1430 UT (Fig. 34.3, lower panel). As a result, the equatorial CEJ occurred, causing an equatorial enhancement of the negative bay at the dayside dip equator, Mokolo (Fig. 34.1). It is to be noted that the shielding electric field, i.e., the R2 FACs started to increase at around the onset of the substorm and continued growing during the expansion phase. When the IMF turned northward during the expansion phase, the well-grown R2 FACs cause a large amplitude CEJ (Kikuchi et al., 2003). Figure 34.4 shows a schematic diagram of the current circuit between the inner magnetosphere and the ionosphere at the dayside dip equator during the period of overshielding in substorm expansion phase. The R2 FACs and the equatorial CEJ are connected by the Pedersen current at mid and low latitudes.

34.4 DP2 Currents and CEJ During Geomagnetic Storms

During the storm main phase, intense dawn-to-dusk electric field is generated deep inside the magnetosphere, which would cause equatorward shift

Fig. 34.2 The Hall and Pedersen conductivities (*upper panel*), NS and EW components of the electric field (*middle panel*) observed by EISCAT (66.16° CGM Lat), and the X component magnetic field at Nurmijarvi measured from the quiettime level. The correlation coefficients, $r(E-X)$, are calculated between the NS electric field at EISCAT and X-component at Nurmijarvi during the growth phase (DP2) and expansion phase of the substorm. (figure 6 of Kikuchi et al. (2000), reproduced by permission of American Geophysical Union)

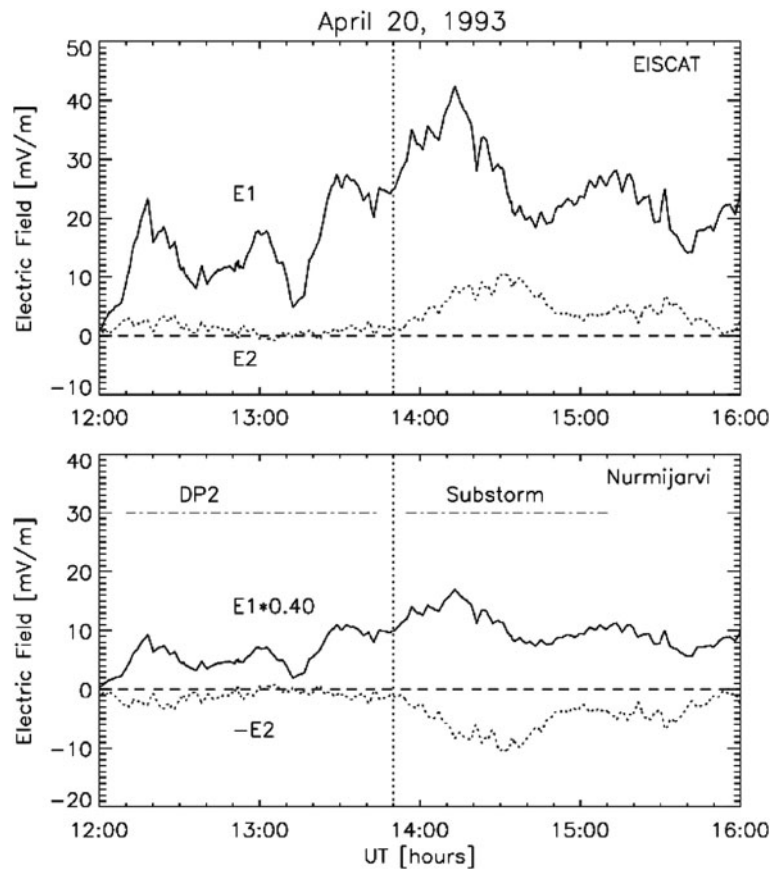


of auroral electrojet to mid latitude (Feldstein et al., 1997). The stormtime electric field penetrated to the inner magnetosphere as observed by CRRES and Akebono satellites at $L = 2-6$ (Wygant et al., 1998; Burke et al., 1998; Shinbori et al., 2005), driving the storm ring current. Shinbori et al. (2005) demonstrated temporal variations of the convection electric field at a distance of 2–5 R_E during the main phase of the major storm on March 13, 1989, with maximum magnitude of 46 mV/m.

Wilson et al. (2001) demonstrated that the DP2 currents developed at mid latitude during a geomagnetic storm, when a significant electric field was detected by CRRES inside the ring current. They suggested that the electric field associated with the DP2 currents might have contributed to the development of the storm ring current. The convection electric field further penetrates to the equatorial ionosphere, driving the DP2 currents and intensifying the equatorial EEJ (Tsurutani et al., 2004; Huang et al., 2005; Kikuchi et al., 2008a, b).

Kikuchi et al. (2008a) analyzed a geomagnetic storm recorded at the dayside dip equator, Yap (YAP, -0.3° GM Lat), off equator, Guam (GAM, 4.89° GM Lat) and low latitude, Okinawa (OKI, 14.47° GM Lat) as shown in Fig. 34.5. The temporal variations at OKI indicate those of the ring current, which developed immediately after the storm sudden commencement (SC) because of the strong southward IMF. The storm at YAP, on the other hand, increased considerably for more than 1 h during the main phase, while decreased considerably during the recovery phase. As a result, the geomagnetic storm was enhanced at the equator with an equatorial to low latitude amplitude ratio of 2.7. Rastogi (2004) demonstrated that the magnitude of the geomagnetic storm was significantly enhanced at the dayside dip equator, which was attributed to the CEJ caused by the northward turning of the IMF. Kikuchi et al. (2008a) pointed out that the geomagnetic storm was enhanced by a combined effect of the DP2 currents during the main phase and the CEJ during the recovery phase.

Fig. 34.3 Estimated electric fields associated with the R1 and R2 FACs at EISCAT ($E1$, $E2$) and at Nurmijärvi ($E1 \times 0.4$, $-E2$) during the growth (DP2) and expansion phases of the substorm, deduced from the electric field measured by EISCAT and the X-component magnetic field at Nurmijärvi (Fig. 34.2). (figure 8 of Kikuchi et al. (2000), reproduced by permission of American Geophysical Union)



Difference between YAP and OKI provides us with DP2/CEJ during the storm, which is shown in the bottom panel of Fig. 34.6 together with contours of westward auroral electrojet derived from the IMAGE magnetometer data at the dawn sector (upper panel). The DP2 currents are remarkably enhanced during the main phase (02–04 UT), but it changes to CEJ during the recovery phase (04–07 UT). The auroral electrojet developed during the main phase at mid latitude (57° CGM Lat), but it shifted poleward rapidly to the normal auroral latitude (67° CGM Lat) at the beginning of the recovery phase. Huang et al. (2005) pointed out that the convection electric field continued to penetrate to low latitude for many hours during the whole period of storm main phase. This tendency is observed in Fig. 34.6, but the DP2 started to decrease at 0250 UT, indicating that the shielding became effective in late main phase (Kikuchi et al., 2008a). The AEJ was intensified over 0240–0340 UT with a peak at 0310 UT, when the equatorial DP2 was decreasing its intensity. The distinct temporal behavior at the two latitude

regions implies development of the R2 FACs below 55° CGM Lat, which intensifies/reduces the electric field at auroral/lower latitude. Because of the developing R2 FACs, overshielding occurred at the beginning of storm recovery phase, when the convection electric field decreased because of a decrease in the southward IMF (Kikuchi et al., 2008a). The overshielding electric field responsible for the CEJ would be transmitted to the inner magnetosphere, where the ring current must have ceased developing because of the reversed electric field. The reversed electric field was observed by CRRES during the storm recovery phase (Wygant et al., 1998). These observations imply that the electric field associated with the DP2 currents contributes to the ring current development, while the overshielding electric field may contribute to the decay of the ring current.

The stormtime current circuits are composed of the R1 FAC-DP2 during the main phase and the R2 FAC-CEJ during the recovery phase, which are similar to those of the substorm growth and expansion

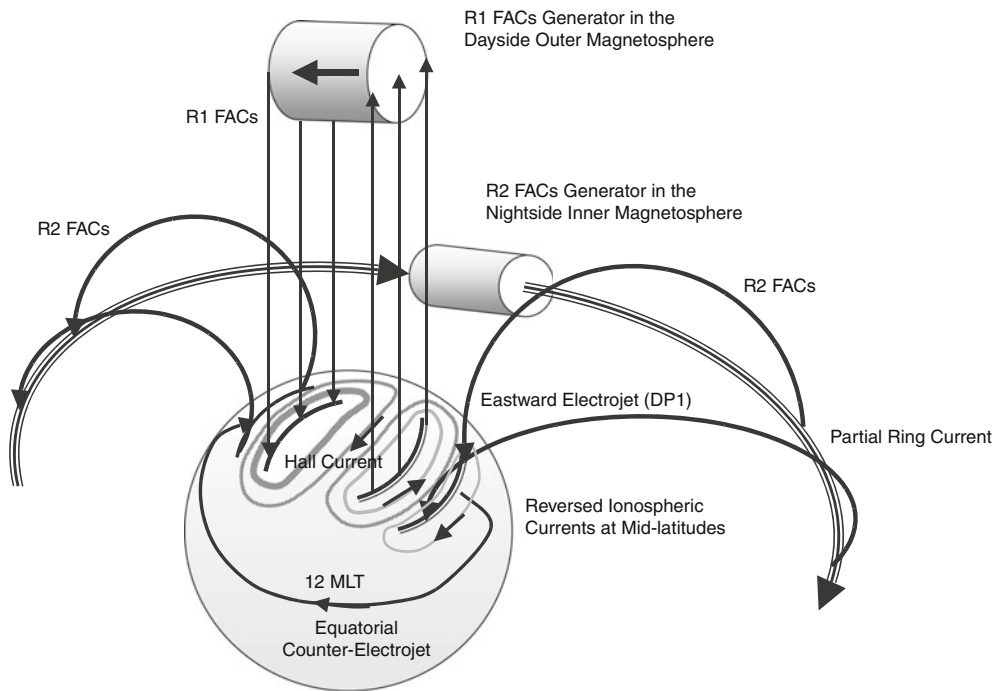


Fig. 34.4 Schematic diagram of the current system in the magnetosphere and ionosphere during the substorm. The R1 and R2 FACs flow into the equatorial ionosphere through the polar ionosphere, resulting in the equatorial DP2 during the growth phase,

while the equatorial CEJ appears during the expansion phase. The diagram is pertinent to the equatorial CEJ. (figure 11 of Kikuchi et al. (2003), reproduced by permission of American Geophysical Union)

Fig. 34.5 H-component magnetic fields recorded at low latitude, Okinawa (OKI, 14.47° GML), and near the dip equator, Guam (GAM, 4.89° GM Lat), and Yap (YAP, -0.3° GM Lat) during the storm on November 6, 2001. The stations were located at around noon when the storm started (MLT=UT+9). (figure 6 of Kikuchi et al. (2008a), reproduced by permission of American Geophysical Union)

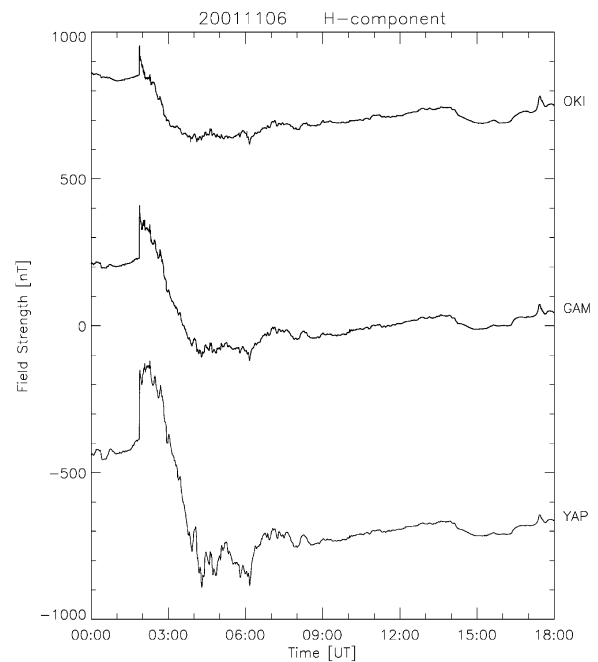
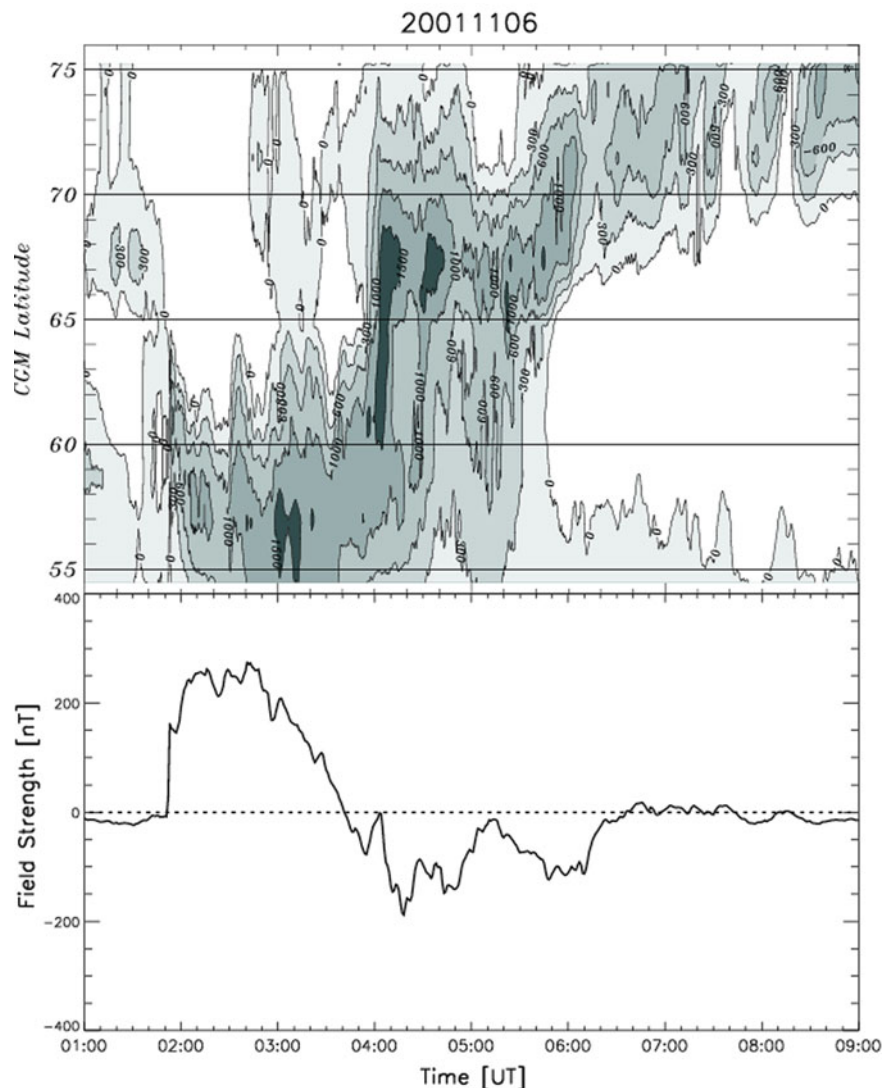


Fig. 34.6 (*Upper panel*): Contour map of the magnetic disturbances caused by the westward electrojet at auroral – mid latitudes in the dawn sector derived from the IMAGE magnetometer array data. (*Lower panel*): Magnetic deflections caused by storm-time ionospheric currents at YAP obtained by subtracting magnetic disturbances at OKI after eliminating quiettime diurnal variations on November 4, 2001. The magnetic disturbance at OKI is used to eliminate effects of the magnetospheric currents. (figure 8 of Kikuchi et al. (2008a), reproduced by permission of American Geophysical Union)



phases, respectively. Kikuchi et al. (2008b) confirmed the current circuits of the main and recovery phases, by analyzing two other storm events with different conditions of the IMF. The rapid poleward shift of the auroral electrojet was commonly observed in the three events, which must be related to reconfiguration of the magnetosphere during substorms. The role of the substorm in the evolution of the geomagnetic storm remains a crucial issue in the storm-substorm relationship.

It should be noted that the CEJ was observed even during the storm main phase. Fejer et al. (2007) indicated that the electric field at the equator was opposite in direction to that of the convection electric field on

both the day- and night-sides for the storm event on November 10, 2004. On the other hand, the electric field was the normal convection electric field during the storm main phase on November 9, 2004. The disturbance dynamo caused by the thermospheric wind (Blanc and Richmond, 1980) must have been activated by the first storm, of which electric field overcame the convection electric field in main phase of the second storm. It should be reminded that the disturbance dynamo starts to work with a time lag of several hours from the beginning of storm and continues to work for a long time, say, 10 h (Fejer and Scherliess, 1997). The overshielding electric field is caused by the R2 FACs flowing into the auroral ionosphere, while the

disturbance dynamo works in the mid latitude thermosphere. Latitude and local time distribution of the ionospheric electric field will enable us to distinguish the overshielding electric field from that of the disturbance dynamo.

34.5 Electric Field Transmission Mechanism

The near-instantaneous transmission of the convection electric field to the equator was first suggested by Araki (1977), based on his finding of the simultaneous onset of the preliminary reverse impulse (PRI) of SCs at high latitude and dip equator with a temporal resolution of 10 s. The ionospheric current pattern of the PRI is about the same as that of the DP2 (Nagata and Abe, 1955; Nishida et al., 1966), driven by a dusk-to-dawn electric field. The PRI electric field was directly observed by HF Doppler measurements as a downward/upward motion of low latitude ionosphere on the day/nightside (Kikuchi et al., 1985). The

PRI electric field is a potential electric field same as the DP2, propagating near-instantaneously to low latitude within 10 s (Kikuchi, 1986). The simultaneity within 10 s is explained by means of the TM_0 mode wave propagating at the speed of light in the Earth-ionosphere waveguide (Kikuchi et al., 1978; Kikuchi and Araki, 1979).

Figure 34.7 shows a schematic diagram of the three-layered Earth-ionosphere waveguide where a downward FAC is given at one end of the waveguide (Kikuchi, 2005). The electric field carried along the FAC is subject to reflection at the ionosphere. However, a fraction of the electric field is transmitted into the Earth-ionosphere waveguide, providing a vertical electric field, E_z below the ionosphere. The vertical electric field excites the TM_0 mode wave, which propagates horizontally (x -direction) at the speed of light, accompanying a magnetic field, H_y transverse to the propagation plane. Thus, the Poynting flux, S_x composed of E_z and H_y is transmitted to low latitude (x -direction). The TM_0 mode wave accompanies electric currents in the ionosphere and at the surface of the ground, which are connected by the displacement

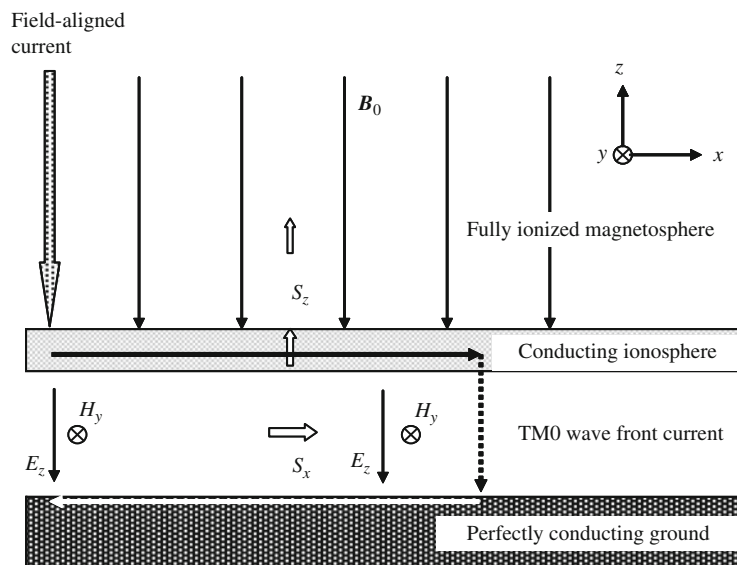


Fig. 34.7 Three-layered Earth-ionosphere waveguide composed of the magnetosphere, ionosphere and neutral atmosphere terminated by the perfectly conducting ground. The TM_0 mode wave propagates in x -direction in the waveguide, characterized by the magnetic field, H_y , transverse to the propagation plane (x - z plane) and vertical electric field, E_z , in the plane. The TM_0 mode wave carries electric currents in the

ionosphere and on the ground, connected by the displacement current at the wave front. The Poynting flux, S_x , composed of E_z and H_y transmits horizontally to low latitude (x -direction). A fraction of energy, S_z , escapes vertically into the ionosphere and the magnetosphere, which will cause quick response of the low latitude ionosphere and prompt development of the electric field in the inner magnetosphere

current at the wave front. The TM_0 mode wave is applied not only to the short-term electric field of the PRI, but also to long lasting electric fields of the DP2 and storm/substorms, because the TM_0 mode wave has no lower cutoff frequency (Kikuchi and Araki, 1979).

A fraction of the Poynting flux is transmitted from the ionosphere to the inner magnetosphere as shown in Fig. 34.7, causing attenuation of the TM_0 mode wave. However, the attenuation is much less than that of the geometrical attenuation due to the finite size of the polar cap electric field even under the nighttime ionospheric condition (Kikuchi and Araki, 1979; Kikuchi, 2005). Under a daytime ionospheric condition with high ionospheric conductance to Alfvén conductance ratio (>10), the electric field associated with the ionospheric current is transmitted by the Alfvén wave upward along the field lines with no appreciable attenuation. The polarization current at the wave front of the Alfvén wave exerts a $\mathbf{J} \times \mathbf{B}$ force on plasma in the F-region ionosphere and in the inner magnetosphere. This results in the coherent variations in the ground magnetic field and in the F-region ionosphere at the geomagnetic equator, as observed by the HF Doppler measurements (Abdu et al., 1998) and by the Jicamarca incoherent scatter radar (Kikuchi et al., 2003). The upward transmission of the Poynting flux would cause the quick development of the electric field in the inner magnetosphere (Nishimura et al., 2009), ring current (Hashimoto et al., 2002), plasmasheet thinning (Hashimoto and Kikuchi, 2005), and reconfiguration of the plasmopause (Murakami et al., 2007).

34.6 Conclusion

1. The convection electric field is transmitted by the Alfvén wave from the dynamo in the outer magnetosphere to the polar ionosphere, accompanying the Region-1 field-aligned currents and driving the DP2 currents composed of ionospheric Hall currents at high latitude and the Pedersen currents amplified by the Cowling effect at the dip equator.
2. The convection electric field is transmitted to low latitude near-instantaneously, resulting in high coherency of the DP2 fluctuations and simultaneous enhancement of the equatorial electrojet during storm/substorms.
3. The electric field associated with the DP2 currents is transmitted into the F-region ionosphere and into the inner magnetosphere, causing quick response of the low latitude ionosphere and ring current development during storm/substorms.
4. The overshielding electric field due to the Region-2 field-aligned currents causes reversal of the ionospheric currents at mid latitude and the counter-electrojet at the dip equator during substorm expansion phase and storm recovery phase.
5. The TM_0 mode wave propagating at the speed of light in the Earth-ionosphere waveguide carries the polar electric field to low latitude near-instantaneously and further into the inner magnetosphere with a time delay no greater than the propagation time of the Alfvén wave.

References

- Abdu MA, Sastri JH, Luhr H, Tachihara H, Kitamura T, Trivedi NB, Sobral JHA (1988) DP 2 electric field fluctuations in the dusk-time dip equatorial ionosphere. *Geophys Res Lett* 25:9. doi:10.1029/98GL01096
- Araki T (1977) Global structure of geomagnetic sudden commencements. *Planet Space Sci* 25:373–384
- Baker WG, Martyn DF (1953) Electric currents in the ionosphere I. The conductivity. *Phil Trans R Soc Lond Ser A* 246:281–294
- Blanc M, Richmond AD (1980) The ionospheric disturbance dynamo. *J Geophys Res* 85:1669–1686
- Burke WJ, Maynard NC, Hagan MP, Wolf RA, Wilson GR, Gentile LC, Gussenhoven MS, Huang CY, Garner TW, Rich FJ (1998) Electrodynamics of the inner magnetosphere observed in the dusk sector by CRRES and DMSP during the magnetic storm of June 4–6, 1991. *J Geophys Res* 103(A12):29,339–29,418
- Dungey JW (1961) Interplanetary magnetic field and the auroral zones. *Phys Rev Lett* 6:47
- Fejer BG, Gonzales CA, Farley DT, Kelley MC (1979) Equatorial electric fields during magnetically disturbed conditions 1. The effect of the interplanetary magnetic field. *J Geophys Res* 84:5797–5802
- Fejer BG, Jensen JW, Kikuchi T, Abdu MA, Chau JL (2007) Equatorial ionospheric electric fields during the November 2004 magnetic storm. *J Geophys Res* 112:A10304. doi:10.1029/2007JA012376
- Fejer BG, Scherliess L (1997) Empirical models of storm time equatorial zonal electric fields. *J Geophys Res* 102(A11):24,047–24,056
- Feldstein YI, Grafe A, Gromova LI, Popov VA (1997) Auroral electrojets during geomagnetic storms. *J Geophys Res* 102:14223–14235
- Gonzales CA, Kelley MC, Fejer BG, Vickrey JF, Woodman RF (1979) Equatorial electric fields during magnetically

- disturbed conditions 2. Implications of simultaneous auroral and equatorial measurements. *J Geophys Res* 84:5803–5812
- Hashimoto KK, Kikuchi T (2005) Quick response of the near-earth Magnetotail to changes in the interplanetary magnetic field. In: Pulkkinen TI, Tsyganenko NA, Friedel RHW (eds) *The inner magnetosphere: physics and modeling*. Geophysical monograph series, vol 155. AGU, Washington, DC, pp 47–53
- Hashimoto KK, Kikuchi T, Ebihara Y (2002) Response of the magnetospheric convection to sudden interplanetary magnetic field changes as deduced from the evolution of partial ring currents. *J Geophys Res* 107(A11):1337. doi:10.1029/2001JA009228
- Hirono M (1952) A theory of diurnal magnetic variations in equatorial regions and conductivity of the ionosphere E region. *J Geomag Geoelectr Kyoto* 4:7–21
- Huang C-S, Foster JC, Kelley MC (2005) Long-duration penetration of the interplanetary electric field to the low-latitude ionosphere during the main phase of magnetic storms. *J Geophys Res* 110:A11309. doi:10.1029/2005JA011202
- Iijima T, Nagata T (1972) Signatures for substorm development of the growth phase and expansion phase. *Planet Space Sci* 20:1095–1112
- Iijima T, Potemra T (1976) The amplitude distribution of field-aligned currents at northern high latitudes observed by Triad. *J Geophys Res* 81:13. doi:10.1029/JA081i013p02165
- Iijima T, Potemra T (1978) Large-scale characteristics of field-aligned currents associated with substorms. *J Geophys Res* 83:A2. doi:10.1029/JA083iA02p00599
- Jaggi R, Wolf R (1973) Self-consistent calculation of the motion of a sheet of ions in the magnetosphere. *J Geophys Res* 78(16):2852–2866
- Kamide Y, Sun W, Akasofu S-I (1996) The average ionospheric electrodynamics for the different substorm phases. *J Geophys Res* 101:A1. doi:10.1029/95JA02990
- Kelley MC, Fejer BG, Gonzales CA (1979) An explanation for anomalous equatorial ionospheric electric fields associated with a northward turning of the interplanetary magnetic field. *Geophys Res Lett* 6:301–304
- Kikuchi T (1986) Evidence of transmission of polar electric fields to the low latitude at times of geomagnetic sudden commencements. *J Geophys Res* 91:3101–3105
- Kikuchi T (2005) Transmission line model for driving plasma convection in the inner magnetosphere. In: Pulkkinen TI, Tsyganenko NA, Friedel RHW (eds) *The inner magnetosphere: physics and modeling*. Geophysical monograph series, vol 155. AGU, Washington, DC, pp 173–179
- Kikuchi T, Araki T (1979) Horizontal transmission of the polar electric field to the equator. *J Atmos Terr Phys* 41:927–936
- Kikuchi T, Araki T, Maeda H, Maekawa K (1978) Transmission of polar electric fields to the equator. *Nature* 273:650–651
- Kikuchi T, Hashimoto KK, Kitamura T-I, Tachihara H, Fejer B (2003) Equatorial counter-electrojets during substorms. *J Geophys Res* 108(A11):1406. doi:10.1029/2003JA009915
- Kikuchi T, Hashimoto KK, Nozaki K (2008a) Penetration of magnetospheric electric fields to the equator during a geomagnetic storm. *J Geophys Res* 113:A06214. doi:10.1029/2007JA012628
- Kikuchi T, Hashimoto KK, Nozaki K (2008b) Storm phase dependence of penetration of magnetospheric electric fields to mid and low latitudes. In: Kintner PM Jr, Coster AJ, Fuller-Rowell T, Mannucci AJ, Mendillo M, Heelis R (eds) *Midlatitude ionospheric dynamics and disturbances*. Geophysical Monograph Series, vol 181. AGU, Washington, DC, pp 145–155
- Kikuchi T, Ishimine T, Sugiuchi H (1985) Local time distribution of HF Doppler frequency deviations associated with storm sudden commencements. *J Geophys Res* 90:4389–4393
- Kikuchi T, Luehr H, Schlegel K, Tachihara H, Shinohara M, Kitamura T-I (2000) Penetration of auroral electric fields to the equator during a substorm. *J Geophys Res* 105:23251–23261
- Kikuchi T, Lühr H, Kitamura T, Saka O, Schlegel K (1996) Direct penetration of the polar electric field to the equator during a DP2 event as detected by the auroral and equatorial magnetometer chains and the EISCAT radar. *J Geophys Res* 101:17161–17173
- Kobe A, Amory-Mazaudier C, Do JM, Luehr H, Houghninau E, Vassal J, Blanc E, Curto JJ (1998) Equatorial electrojet as part of the global circuit: a case-study from the IEEY. *Ann Geophys* 16:698–710
- Kobe A, Richmond AD, Emery BA, Peymirat C, Luehr H, Moretto T, Hairston M, Amory-Mazaudier C (2000) Electrodynamic coupling of high and low latitudes: observations on May 27, 1993. *J Geophys Res* 105(A10):22979–22989
- Matsushita S, Balsley BB (1972) A question of DP2 magnetic fluctuations. *Planet Space Sci* 20:1259–1267
- Murakami G, Hirai M, Yoshikawa I (2007) The plasmopause response to the southward turning of the IMF derived from sequential EUV images. *J Geophys Res* 112:A06217. doi:10.1029/2006JA012174
- Nagata T, Abe S (1955) Notes on the distribution of SC* in high latitudes. *Rept Ionosph Res Jpn* 9:39–44
- Nishida A (1968a) Geomagnetic DP2 fluctuations and associated magnetospheric phenomena. *J Geophys Res* 73:1795–1803
- Nishida A (1968b) Coherence of geomagnetic DP2 magnetic fluctuations with interplanetary magnetic variations. *J Geophys Res* 73:5549–5559
- Nishida A, Iwasaki N, Nagata T (1966) The origin of fluctuations in the equatorial electrojet: a new type of geomagnetic variation. *Ann Geophys* 22:478–484
- Nishida A, Kamide Y (1983) Magnetospheric processes preceding the onset of an isolated substorm: a case study of the March 31, 1978, Substorm. *J Geophys Res* 88(A9):7005–7014
- Nishimura Y, Kikuchi T, Wygant J, Shinbori A, Ono T, Matsuoka A, Nagatsuma T, Brautigam D (2009) Response of convection electric fields in the magnetosphere to IMF orientation change. *J Geophys Res* 114:A09206. doi:10.1029/2009JA014277
- Peymirat C, Richmond AD, Kobe A (2000) Electrodynamic coupling of high and low latitudes: simulations of shielding/overshielding effects. *J Geophys Res* 105(A10):22991–23003
- Rastogi RG (1977) Geomagnetic storms and electric fields in the equatorial ionosphere. *Nature* 268:422–424
- Rastogi RG (1997) Midday reversal of equatorial ionospheric electric field. *Ann Geophys* 15:1309–1315
- Rastogi RG, Patel VL (1975) Effect of interplanetary magnetic field on ionosphere over the magnetic equator. *Proc Indian Acad Sci* 82:121–141

- Senior C, Blanc M (1984) On the control of magnetospheric convection by the spatial distribution of ionospheric conductivities. *J Geophys Res* 89:261–284
- Shinbori A, Nishimura Y, Ono T, Iizima M, Kumamoto A, Oya H (2005) Electrodynamics in the duskside inner magnetosphere and plasmasphere during a super magnetic storm on March 13–15, 1989. *Earth Planets Space* 57:643–659
- Siscoe GL, Crooker NU, Erickson GM, Sonnerup BUO, Siebert KD, Weimer DR, White WW, Maynard NC (2000) Global geometry of magnetospheric currents inferred from MHD simulations. In: Ohtani S, Fujii R, Hesse M, Lysak RL (eds) *Magnetospheric current systems*. Geophysical monograph series, vol 118. AGU, Washington, DC, pp 41–52
- Somayajulu VV, Reddy CA, Viswanathan KS (1987) Penetration of magnetospheric convective electric field to the equatorial ionosphere during the substorm of March 22, 1979. *Geophys Res Lett* 14:876–879
- Southwood DJ (1977) The role of hot plasma in magnetospheric convection. *J Geophys Res* 82:5512–5520
- Tanaka T (1995) Generation mechanisms for magnetosphere-ionosphere current systems deduced from a three-dimensional MHD simulation of the solar wind-magnetosphere-ionosphere coupling processes. *J Geophys Res* 100:A7. doi:10.1029/95JA00419
- Tanaka T (2007) Magnetosphere–ionosphere convection as a compound system. *Space Sci Rev*. doi:10.1007/s11214-007-9168-4
- Tsurutani B et al (2004) Global dayside ionospheric uplift and enhancement associated with interplanetary electric fields. *J Geophys Res* 109:A08302. doi:10.1029/2003JA010342
- Vasyliunas VM (1972) The interrelationship of magnetospheric processes. In: McCormac BM (ed) *Earth's magnetospheric processes*. Reidel, Norwell, Massachusetts, pp 29–38
- Wilson, GR, Burke WJ, Maynard NC, Huang CY, Singer HJ (2001) Global electrodynamics observed during the initial and main phases of the July 1991 magnetic storm. *J Geophys Res* 106(A11):24517–24539
- Wygant J, Rowland D, Singer HJ, Temerin M, Mozer F, Hudson MK (1998) Experimental evidence on the role of the large spatial scale electric field in creating the ring current. *J Geophys Res* 103(A12):29527–29544. doi:10.1029/98JA01436